Numerical analysis of pile foundations and tunnel-pile interaction

by

Tang Ji Jian (CHU)

Fourth-year undergraduate project

in Group D, 2013/2014

"I hereby declare that, except where specifically indicated, the work submitted herein is my own original work."

Technical abstract: Numerical analysis of pile foundations and tunnel-pile interaction

TANG Ji Jian, CHURCHILL College

In line with the pace of urban development, the excavation of tunnels in close proximity to piled structures is increasingly commonplace. Usually, structure foundations are only designed to take loadings from the building above. Nearby tunnel construction could compromise the structural integrity of the buildings above. This requires engineers to be able to predict the interactions between tunnels and piles. Conventional modelling methods tend to be computationally expensive. Thus there is a need for a reliable efficient method to model the effects of tunnelling on foundation settlements.

In this report, the author explores the feasibility and reliability of using a simplified method to predict the effect of tunnelling-induced ground settlements on nearby piled structures.

To develop this tool, a review of recent state-of-the-art research is carried out. The simplified model adopts the Two Step Analysis Method (TSAM). The tunnelling-induced surface and subsurface settlements are first approximated by a widely used empirical Gaussian relation. The pile is discretised into elastic elements through the Finite Element Method (FEM), while the pile-soil interface is assumed to behave elastic-plastically (bi-linear) and discretised according to the Boundary Element Method (BEM). The ground settlements are then imposed onto the discretised elements, followed by the application of an external vertical force on the pile head. The displacements of all nodes are solved iteratively.

A simple parametric test is done on the model to ensure that it is working as expected. The model is then validated against a field test observation of a single loaded pile. The model's prediction matched the field observation very closely.

Further parametric studies are carried out to explore the model's capabilities. The soil, pile, and tunnel parameters were tested rigorously and the results were found to be within expectations.

The model is then validated against field observations obtained by Selemetas (2005). The model's prediction of pile settlements before tunnelling is found to disagree with the field observations. Further investigation is carried out and the source of discrepancy is pin pointed to the model's implementation of the widely used β-method. It is suggested that the β-method might not be suitable for this analysis as no other sources of discrepancies could be located.

The numerical model is found to accurately predict the behaviour of a pile installed in layered clay. However, there are some potential limitations with the model's implementation of the β-method. From the parametric studies in uniform clay, the results are found to agree qualitatively with field observations.

There are a lot of areas that can potentially be worked on in the future. The model's implementation of the β-method requires further inspection. It is recommended that the cyclic non-linear load transfer method is adopted to model the pile-soil interface.

Contents

List of notations

A_p	Pile cross sectional area
$\mathbf{B}$	Strain-displacement matrix
$\mathbf{D}$	Stress-strain matrix
D_t	Tunnel diameter
E_{pile}	Pile elastic modulus
E_{soil}	Soil elastic modulus
$\{f\}$	Vector of input loads
G	Soil shear modulus
i	Settlement trough width
K	Trough width parameter
K_0	Coefficient of earth
$\mathbf{k}_e$	Element stiffness matrix
K_{global}	Global stiffness matrix
K_{pile}	Pile stiffness matrix
K_{soil}	Soil stiffness matrix
L	Pile length
L_e	Pile element length
N_c	Base adhesion factor
P	Imposed vertical load on pile head
r_p	Pile radius
r_m	Distance from pile centre where displacements are negligible
R	Relative settlement between pile and ground
S	Vertical ground settlement due to tunnelling
S_{max}	Vertical ground settlement above tunnel due to tunnelling
s_u	Soil undrained shear strength
v_l	Volume loss (%)
V_s	Volume loss per metre
z_0	Tunnel axis depth
$\{u\}$	Vertical displacement vector
$\{u_t\}$	Vector of ground movements due to tunnelling
α	Shaft adhesion factor
β	$k_0 \tan(\delta)$
δ	Pile-soil friction angle
ε	Strain
γ	Soil unit weight
$[\lambda_{soil}]$	Soil flexibility matrix
ν	Poisson's ratio

ϕ_{crit}	Critical friction angle
ϕ_{peak}	Peak friction angle
σ'_{v0}	Effective vertical stress
τ_0	Pile-soil interface shear stress

1 Introduction

Half of the world's population now live in urban areas. In line with the increasing density of urban areas all around the world, underground metro systems and motorways are constantly being built to ease congestion. As tunnel construction has a measurable impact upon the soil around the tunnel, existing foundations in close proximity to the tunnel will also be affected. Engineers need to be able to predict such effects sufficiently accurately to ensure the safety of infrastructure both above and below ground.

Since foundations are initially designed to support only the structures above it, they are likely to be adversely affected by nearby ground disturbance. The exercise of predicting the likely damage, inflicted upon structures founded on shallow foundations, is relatively straightforward. Equations describing the interaction between ground settlement and building settlement are readily available.

On the other hand, deep foundations i.e. piled foundations tend to exhibit a more complicated behaviour when subjected to ground deformations. This is because ground settlement is not uniform with depth, hence piles will experience varying amounts of soil movement along the depth. Furthermore, the many layers of soil, each with its own properties, pose another challenge to analysis. These interactions will cause the foundation to settle as well as induced additional loading on the piles. This remains an area of active research, and the interaction between tunnel linings and nearby piles is still being investigated. The degree of uncertainty compels engineers to take extra precaution and adopt higher factors of safety, which in turn translates into expensive building protection procedures.

It is common practice in the industry to model the problem using continuum finite element analysis. However this approach is computationally expensive, requiring hours to obtain results, and is also susceptible to changes in boundary conditions [citation needed].

In this project, a simplified model to analyse tunnel-pile interactions will be examined. To develop and test this model, a general study was conducted on pile settlements, tunnelling-induced ground settlements, tunnelling effects on piles, and finite element analysis.

The model is expected to be computationally fast because several assumptions are made. The simulated pile is modelled to be supported by multiple springs along the length, with one end of each spring attached to the pile, and the other end to a rigid ground. The springs are made to simulate the pile-soil interaction at the pile-soil interface, undoubtedly with simplifications. The effect of tunnelling is simulated by imposing the ground settlements due to tunnelling on the ground end of the springs. The underlying assumption is that the ground settlements due to tunnelling are not affected by the presence of a pile.

The tool is then tested and compared against experimental data to examine the validity of the assumptions.

Problem statement Piled foundations are designed to take loading only from the structure above. Nearby tunnel construction will affect the foundation's performance. Current analysis conventions are computationally expensive. Is it feasible to use simplified methods of numerical finite element analysis to model the effect of tunnelling on foundation settlements? If yes, is it reliable?

Approach to the solution A simplified beam-spring model (Chapter 3) is used to simulate tunnel-pile interactions. The model is tested parametrically and validation against field data is carried out.

1.1 Aims and objectives

The objective of this project is to review the state of the art in current literature and evaluate the applicability and reliability of simplified methods of numerical finite element analysis.

1.2 Structure of report

Following this introductory chapter, Chapter 2 offers an overview of previous studies on piled foundations, soil settlements from tunnel construction, and effects of tunnelling on nearby piles, concluding with a brief discussion.

Chapter 3 describes the development process of the analysis tool. It includes an example of the tool's prediction of a fictional case study.

Chapter 4 presents comparisons between the analysis tool's prediction and field data, as well as results from parametric studies of the tool.

Chapters 5 and 6 outline, respectively, the findings of this study and recommended areas to be worked on.

2 Literature review

This section summarises research in pile behaviour, 'greenfield' tunnel settlements, and the effects of tunnelling on nearby piles. A discussion of previous studies is presented at the end of the chapter.

2.1 Settlement of piled foundations

Deep foundations, i.e. piled foundations, are used to transfer the loads from a structure into deeper soil, which is usually stiffer and stronger.

Due to the complex interactions between the piles, soil, and raft, various simplifying assumptions have to be made in order to predict the settlement of a piled foundation. In the past, the settlement is often estimated by assuming that the structure rests on an equivalent raft that is situated at two-thirds of the depth of piles.

With improved computing capabilities, the problem can be analysed numerically through finite element analysis or finite difference method. Due to the level of precision needed for these kinds of analyses, long computation times are often required to obtain results.

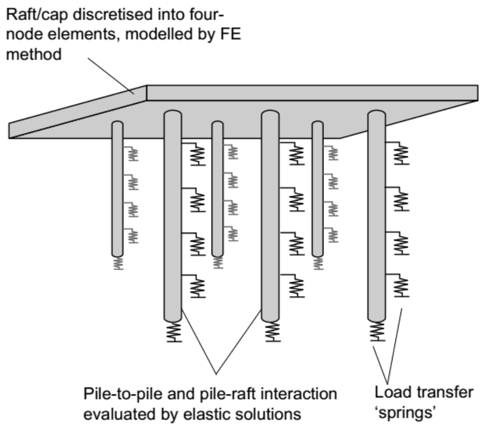

Figure 1: Schematic of simplified method that adopts the boundary element method to model the soil (Leung, 2010).

Simplified models have been developed to reduce computation complexity. A common approach is to adopt the boundary element method, through which only the foundation and the pile-soil interface are discretised. The soil is modelled as an elastic continuum (Mindlin, 1936) rather than discrete elements (figure 1). This greatly reduces the size of the matrix involved in the solution, thus saving computing effort.

Poulos and Davis (1968) used the aforementioned approach to study single incompressible piles. Chow (1986) incorporated the compressibility of piles by expressing pile stiffness in a pile stiffness matrix $[K_{pile}]$ and separately the pile-soil interface by a soil stiffness matrix $[K_{soil}]$. Displacements ($\{u\}$) of the system can be found by solving the following equation:

$$([K_{pile}] + [K_{soil}])\{u\} = \{f\} \tag{1}$$

where $\{f\}$ is the vector of input forces.

This approach fails at higher soil strains as soil is an inherently non-linear material. A simple way to incorporate this is to limit the allowable shear stress at a yielding node. This is known as the 'elastic-plastic' interface model (Poulos, 1989). The limiting frictional shear stress that can be taken by the pile shaft is given by $\tau = \alpha s_u$ in clay and $\tau = \beta\sigma'$ in sand or gravel (Craig, 2004).

This study will focus on axially loaded piles using the 'elastic-plastic' interface model. Further description is included in Chapter 3.

2.2 Tunnelling-induced ground movements

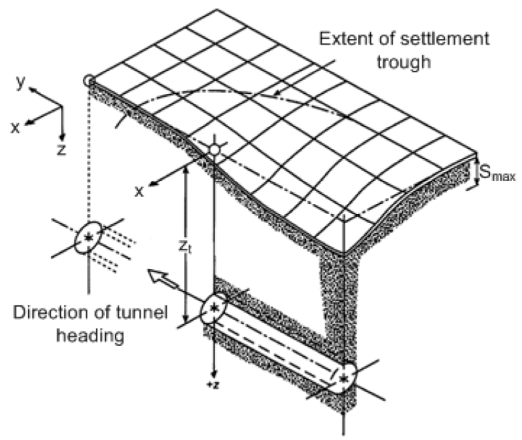

Figure 2: Settlement above advancing tunnel (Attewell et al., 1986).

The cross section of the surface settlement profile far away from the excavation face is well described by an inverse Gaussian curve (Peck, 1969). This is commonly referred to as the 'greenfield' settlement, when the settlement trough is not affected by nearby structures. On the other hand, the longitudinal settlement profile above the tunnel near the excavation face takes the form of a cumulative probability curve. The settlement profiles could be found using analytical solutions, field observations (Cording and Hansmire, 1975), centrifuge modelling (Mair, 1978), and numerical analysis.

Analytical solutions

The shape of the settlment trough was solved analytically by Sagaseta (1987). The following equation is suggested to describe the settlement trough:

$$S(x, y) = \frac{v}{2\pi} \frac{x}{x^2 + h^2} \left[1 + \frac{y}{\sqrt{x^2 + y^2 + h^2}} \right] \tag{2}$$

where v is the volume loss, h is the depth of the tunnel axis, x is the horizontal distance to the tunnel centre-line, y is the horizontal distance to the tunnel face, perpendicular to x.

Figure 2 shows the developing settlement trough as a tunnel is being excavated underneath.

Verruijt and Booker (1996) and Loganathan and Poulos (1998) similarly offered analytical solutions to 'greenfield' settlements. The solutions provided by Puzrin et al. (2012) and Zymnis et al. (2013) further considered the effects of soil anisotropy.

Numerical studies

Addenbrooke et al. (1998) provided numerical solutions to tunnelling settlements in anisotropic soil (specifically London Clay).

Empirical formulae based on field and experimental data

The Gaussian curve (figure 3) mentioned in the previous section is given as

$$S_v(x) = S_{v,max} \cdot \exp(-x^2/2i^2) \tag{3}$$

where $S_{v,max}$ is the settlement above the tunnel centre-line, x is the transverse distance from the tunnel centre-line, and i is the transverse distance between the point of inflection of the settlement profile and the tunnel centre-line. $S_{v,max}$ is found by

$$S_{v,max} = \frac{v_s}{\sqrt{2\pi}i} \tag{4}$$

where $v_s = v_l \cdot \pi D_t^2/4$ (Peck, 1969). D_t is the tunnel diameter while v_l is the volume loss. v_l is usually in the range of 1–2% when tunnelling in soft clays and 0.5% in sands (Mair and Taylor, 1997). Tunnelling with advanced tunnel boring machines can bring the volume loss down to about 0.2% in stiff London Clay (Selemetas, 2005).

The parameter i describes the width of the settlement trough and is shown to vary linearly with the depth of the tunnel as follows:

$$i(z) = K(z) \cdot (z_0 - z) \tag{5}$$

where z_0 is the depth of the tunnel, z is the depth of interest and K is known as the trough width parameter. K is dependant on soil type, and it is found to be around 0.5 in clay and 0.25 in sand (O'Reilly and New, 1982) at the surface. Thus, tunnelling in sandy soil will result in a much deeper and narrower surface settlement trough compared to tunnelling in clay. Mair and Taylor (1997) suggested that K could be in the range of 0.25–0.45 in sands and 0.4-0.6 in clays.

The subsurface settlement profile is found by first determining the trough width parameter at the depth of interest. However, Mair et al. (1993) highlighted that assuming $K = 0.5$ underestimates the width of the settlement profile near the tunnel crown, hence overestimating the settlement above the tunnel centre-line, $S_{v,max}$. A more accurate equa-

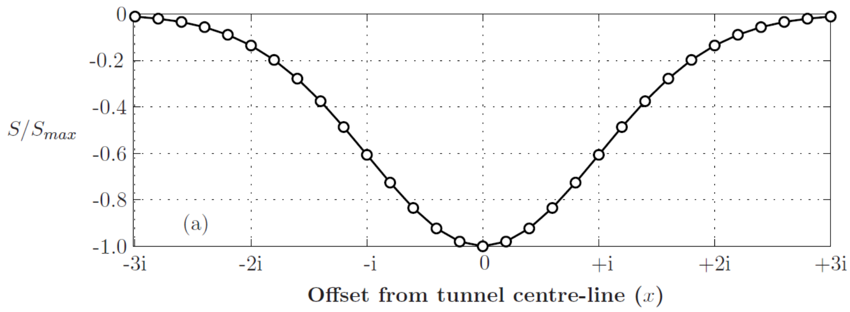

Figure 3: The Gaussian settlement trough as visualised by Selemetas (2005).

tion for K was proposed:

$$K(z) = \frac{0.175 + 0.325(1 - (z/z_0))}{1 - (z/z_0)} \tag{6}$$

Marshall (2009) proposed a modified Gaussian curve that provides a better description of the settlement trough while tunnelling in sand. This is a vast topic, a detailed analysis of which lies beyond of the scope of this study.

In short, the subsurface ground settlement profile becomes wider and shallower, the closer it is to the ground surface.

2.3 Effects of tunnelling on nearby piles

The effects of tunnelling on nearby piles are very complex. Settlement of ground due to tunnelling causes piles to settle in order to mobilise the required shaft friction. It is not uncommon to see tension-inducing negative shaft friction near the pile toe when the tunnel crown is sufficiently near. In serious cases, the pile may even lose much of its capacity and ultimately fail.

Various parameters can affect the performance of piles, including but not limited to volume loss during tunnel construction, pile loading, geometry of the tunnel and the foundation, as well as their relative positions.

To investigate the effects, various methods were used (Jongpradist et al., 2013):

- **Field studies**
  Full scale test piles are instrumented and continuously monitored for changes in stress and strain over the course of tunnel construction. Nearby structures can also be monitored for settlement. Recent examples as follows (Selemetas, 2005):
  - Channel Tunnel Rail Link, Essex: Selemetas (2005)
  - Victoria Line, London: Morgan and Bartlett (1969).
  - North-East Line, Singapore: Coutts and Wang (2000); Yong and Pang (2004); Pang et al. (2005).

  - North/South Line, Amsterdam: Bakker et al. (1999); Teunissen and Hutteman (1998).
  - Rinkai Higoshi-Shinagawa Tunnel: Takahashi et al. (2004).

- **Scaled experiments**
  Scaled test piles are investigated under 1g (Morton and King, 1979) or placed in a centrifuge to simulate realistic stress levels. Recent studies in Cambridge: Jacobsz (2002) and Farrell (2011).

- **Numerical analysis**
  The problem is investigated using a variety of approaches. Two main types of analysis are common:

  - Full 3D analysis. This performs analysis on piles and the surrounding soil, fully modelling the pile-soil interaction. Finite Element Method (FEM) and Finite Difference Method (FDM) are used (Mroueh and Shahrour (2002); Lee and Ng (2005); Lee and Jacobsz (2006); Cheng et al. (2007)).
  - Two stage analysis method. This approach assumes that the 'greenfield' settlement due to tunnelling is not affected by the presence of piles. The model first estimates the 'greenfield' settlement (section 2.2), and then imposes it onto existing piles. Boundary Element Method (BEM) is used (Loganathan et al. (2001); Xu and Poulos (2001)). Kitiyodom et al. (2005) adopted a hybrid approach, by combining FEM and modelling the soil by using interactive springs based on Mindlin (1936).

Most of the experimental studies examined the trends and proposed what is described as an influence zone based on the findings. The influence zone is an area around the tunnel. The settlement of a pile is expected to be large if the pile toe is located within the zone. The influence zone is commonly used as a guide to control the distance between a new tunnel and existing piles.

Early conventions assume that the influence zone (figure 4) is bound by a line that rises from the side of the tunnel at an angle of $(45° + \phi'/2)$ to the vertical (Morton and King, 1979; Attewell et al., 1986), where ϕ' is the friction angle of the soil. Another convention adopts the line that connects the side of the tunnel to a point that is $2.5i$ away from the tunnel centre-line (Cording and Hansmire, 1975; Attewell et al., 1986).

With recent advances in monitoring and experimental techniques, influence zones of different shapes are proposed. The proposal by Lee and Bassett (2007) was based on model tests and numerical analysis. Jacobsz (2002) carried out experiments in a beam centrifuge and proposed an influence zone in sand (figure 5). Using full-scale instrumented piles, Selemetas (2005) was able to investigate the settlement of piles in clay. He proposed

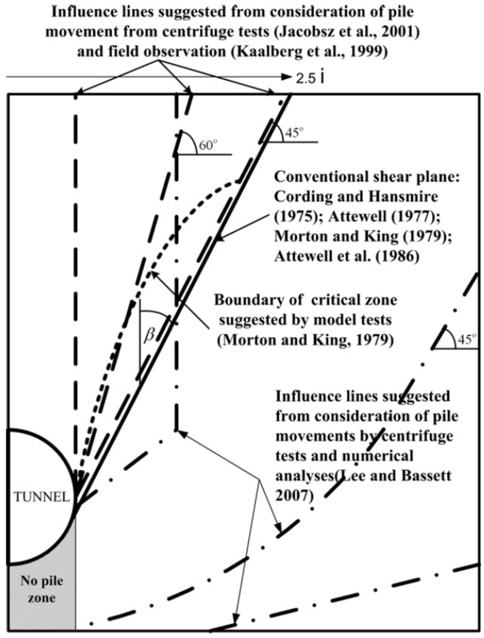

Figure 4: Proposed influence zones (Jongpradist et al., 2013).

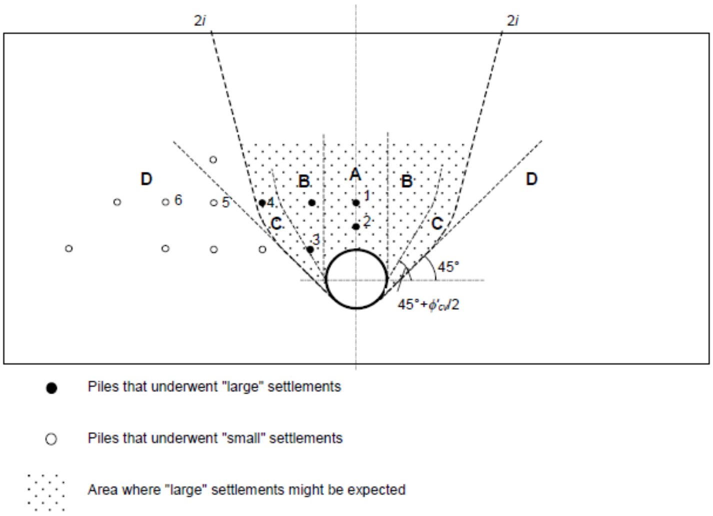

Figure 5: Proposed influence zone (Jacobsz, 2002).

that there are three zones: A, B, and C. The relative pile settlements are expected to be different in each of the three zones, as shown in figure 6.

Jongpradist et al. (2013) carried out an extensive parametric study using FEM and proposed another zoning method based on numerical analysis results. For piles that have their pile toe in Zone I, very large settlements are anticipated and protective measures need to be taken. In Zones I and II, the base load is likely to drop and the pile will settle more to mobilise additional shaft friction. In this case, the piles need to be monitored closely during excavation. The volume loss must also be controlled at a low level. For zone III, the pile settlement is expected to be lower than the ground settlement, and the pile base load should remain the same or slightly higher due to soil settlement at the top.

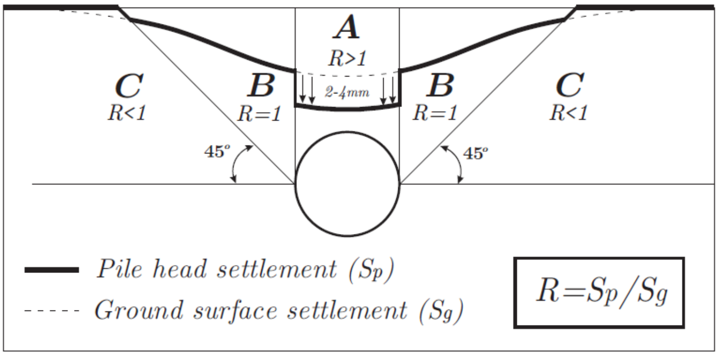

Figure 6: Zones of influence as proposed by Selemetas (2005).

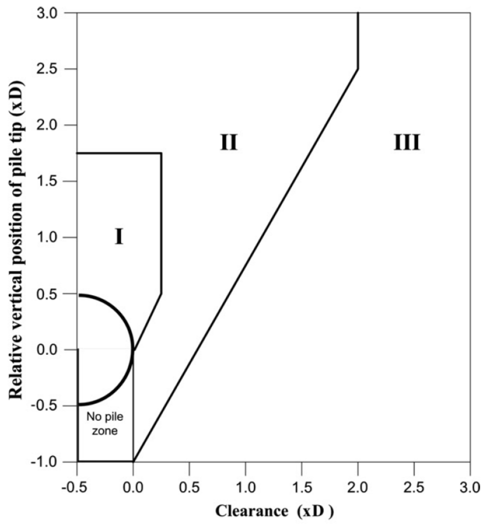

Figure 7: Zones of influence as proposed by Jongpradist et al. (2013).

The studies mentioned above refer to the effects of tunnelling on bored piles. Marshall and Mair (2011) found that, due to the initial locked-in stresses in driven piles (and jacked piles), such piles exhibit a different behaviour. It is suggested not to use 'greenfield' settlements when analysing driven piles.

2.4 Discussion

Useful insights into the current state of research were gleaned from a review of the literature.

In this study, a model to evaluate tunnelling-induced effects on piles is developed. It is to be parametrically tested and validated against field observations by Selemetas (2005) for applicability and reliability.

The model will adopt the two-stage analysis method, by first estimating the likely 'greenfield' ground settlement due to tunnel construction, which is then imposed onto a model of a pile. The pile is discretised into finite elements whereas the surrounding soil is characterised by boundary elements.

3 Development of numerical model

In this section, the development of the model is detailed, followed by an example output for a fictitious scenario.

The planned simplified model will discretise the pile into elastic finite elements. The pile-soil interface is modelled as a bi-linear elastic-plastic boundary element. The model will take the following parameters as input:

- **Load**: a single vertical point load at the top of the pile.
- **Pile**: geometry (length and diameter), material properties (elastic modulus), and relative position to tunnel.
- **Soil**: soil type, depth of soil layer, shear modulus G, Poisson's ratio ν, undrained shear strength s_u, peak friction angle ϕ_{peak}, critical friction angle ϕ_{crit}, soil unit weight γ, K_0, and depth of water table.
- **Tunnel**: depth of tunnel axis z_0, diameter of tunnel $D_t = 2r_t$, volume loss during excavation v_l, and trough width parameter K.
- **Mesh**: defines the size of elements, which in turn dictates the time needed to obtain results.

The simplified model will yield the following output:

- **Displacements**: settlement of all points along the length of the pile.
- **Forces**: axial force along the length of the pile.
- **Ground movement**: displacements of soil due to tunnel construction.

3.1 Finite element method

This subsection delineates the steps taken by the model to derive the necessary variables needed for the analysis.

For a simple case of a pile loaded axially, far away from other structures, the model predicts the pile's settlement, $\{u\}$, by solving:

$$\begin{aligned}[K_{global}]\{u\} &= \{f\} \\ \{u\} &= [K_{global}]^{-1}\{f\}\end{aligned} \tag{7}$$

where $\{f\}$ is the vector of input loads and $[K_{global}]$ is the global stiffness matrix:

$$[K_{global}] = [K_{pile}] + [K_{soil}] \tag{8}$$

$[K_{pile}]$ is the stiffness matrix of the pile. This describes, in the present case, the compressibility of the pile when loaded axially. The model treats each pile element as being supported by a non-linear spring (figure 8) and $[K_{soil}]$ acts as a collection of the spring constants.

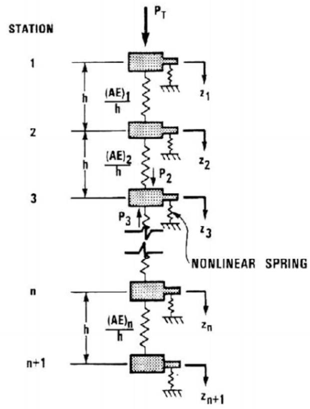

Figure 8: Schematic representation of the load transfer method (Kraft et al., 1981)

Adopting from Zienkiewicz and Taylor (2005), piles are discretised into 1D bar elements, with one degree of freedom at both nodes, for vertical displacement. $[K_{pile}]$ is assembled from the stiffness matrices of each pile element, which have the following general equation:

$$\mathbf{k_e} = \int_{V_e} \mathbf{B}^T \mathbf{D} \mathbf{B} \, dV \tag{9}$$

The pile elements are 1D, 2-node bar elements, $\mathbf{D}$ is simply $E_{pile}A_{pile}$. Hence

$$\mathbf{k_e} = \frac{E_p A_p}{L_e} \begin{bmatrix} 1 & -1 \\ -1 & 1 \end{bmatrix} \tag{10}$$

Assembling the pile elements yield:

$$[K_{pile}] = \frac{E_p A_p}{L_e} \begin{bmatrix} 1 & -1 & 0 & \cdots & 0 \\ -1 & 2 & -1 & \cdots & 0 \\ 0 & -1 & 2 & \cdots & 0 \\ \vdots & \vdots & \vdots & \ddots & -1 \\ 0 & 0 & 0 & -1 & 1 \end{bmatrix} \tag{11}$$

This is because node 2 on element i is shared with node 1 on element $i+1$. Elements are numbered sequentially such that the first element is at the top of the pile. For $[K_{pile,ii}]$, node i starts with 1 at the pile head and increases along the depth of the pile.

Forces and strains in each pile element can be calculated after the analysis, by:

$$\varepsilon_i = \frac{u_{i+1} - u_i}{L_e} \tag{12}$$

$$f_i = E_p A_p \cdot \varepsilon_i \tag{13}$$

These calculations are used when comparing test results against field data, as the results are usually in the form of forces or strains along the length of the pile.

3.2 Modelling of pile-soil interface

Due to its nature as a non-linear material, soil is difficult to model. When sheared, the soil loses its stiffness and eventually shears at a constant shear strength.

For simplicity, pile-soil interactions i.e. the springs are modelled using the elastic-plastic load transfer approach (Klar et al., 2004). The pile-soil interface is modelled to be held together by independent bi-linear springs, each attached to an element. The spring that binds together the pile element and the soil behaves linearly up to a point where it slips at a constant shear stress.

Once a spring reaches its limit, the pile element 'slips' relative to the ground. Any extra loading will have to be transmitted to other springs. This does not model the soil behaviour with exact precision, but it allows the soil to be modelled with relative ease (Leung, 2010).

Assuming linear soil behaviour, the vertical displacement of the pile shaft (Randolph and Wroth, 1978) is:

$$u = \tau_0 r_p \int_{r_p}^{r_m} \frac{dr}{Gr} \tag{14}$$

Integrating equation (14) gives the stiffness of the springs connected to each element (Kraft et al., 1981):

$$\text{Pile-soil stiffness at pile shaft, } K^s_{soil,ii} = \frac{2\pi G L_e}{\ln(r_m/r_p)} \tag{15}$$

$$\text{Pile-soil stiffness at pile base, } K^b_{soil,ii} = \frac{4Gr_p}{1-\nu} \tag{16}$$

where G is the shear modulus of the soil at the depth of the pile element, L_e is the length of the element, and r_p is the pile radius. Numerical analysis suggested that $r_m = 2.5L(1-\nu)$ Leung (2010).

There are two methods to determine the capacity of the shaft springs at the point where it starts to slip: the α-method and the β-method. α-method is used when the soil can be treated as undrained, as in the case of clay. In sands and gravels, the β-method is used.

$$\text{In clayey soil, } P_{fs} = 2\pi r_p L_e \times \alpha s_u \tag{17}$$

$$\text{In sand/gravel, } P_{fs} = 2\pi r_p L_e \times \beta \sigma'_{v0} \tag{18}$$

where $2\pi r_p L_e$ is the surface area of the pile element in contact with soil, s_u is the undrained shear strength of the soil, σ'_{v0} is the vertical effective stress, and $\beta = K_0 \tan\delta$. K_0 is the coefficient of earth pressure and $\tan\delta$ is the soil-pile friction angle. Based on empirical data, α is found to be in the range of 0.4-0.6 in London Clay whereas δ is around 0.75ϕ, ϕ being the friction angle.

For the element at the base of the pile, an additional capacity is provided by the soil directly underneath the element. This is known as the pile base capacity, given by

$$P_{fb} = \pi r_p^2 \times N_c s_u \tag{19}$$

where $N_c = 9$ for deep foundations in clay (Skempton, 1951), and

$$P_{fb} = \pi r_p^2 \times N_q \sigma'_{v0} \tag{20}$$

where N_q is 50 in dense sand.

Once the load capacity of a node is reached, the spring of the relevant node is set to zero stiffness with the load set at the node's capacity. The solving process is iterated with a modified $[K_{soil}]$ until there are no more springs that take a larger load than its capacity (Klar et al., 2007).

The model can assume a constant s_u over a whole layer of clay, or assume a more accurate estimation where the strength increases linearly with depth. A parameter that describes the increase in strength per depth is needed for the more accurate estimation.

The β-method requires the vertical effective stresses in the soil to be known at all depths. Hence the model requires both the unit soil weight and the depth of the water table as inputs to estimate σ'_{v0}.

3.3 Tunnelling settlements

The model generates tunnelling-induced surface and subsurface ground settlements by using the Gaussian functions (section 2.2) as it is easy to implement.

Figure 9 depicts a series of subsurface ground settlement profiles as generated by the model. Vertical settlement is exaggerated by 100 times, otherwise the figure is to scale. A cross section of the tunnel is added as reference (4 m diameter at a depth of 20 m).

As expected, the settlement above the tunnel centre-line, S_{max} increases with depth whereas the settlement profile narrows with depth, as shown by the points of inflection.

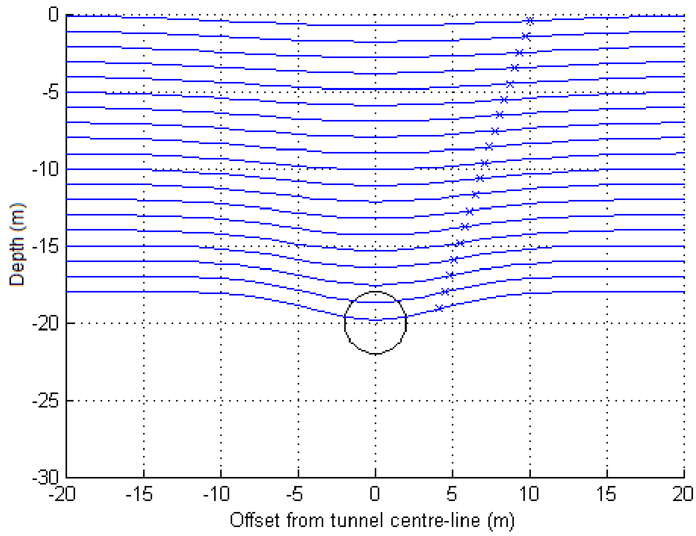

Figure 9: Sub-surface settlements and points of inflection.

In the numerical model, equation (6) is modified. This is to accommodate different surface values of K, as the original equation only works for $K = 0.5$. It is modified to:

$$K(z) = \frac{(K_{surface} - 0.325) + 0.325(1 - (z/z_0))}{1 - (z/z_0)} \tag{21}$$

3.4 Implementation procedure

The model starts the analysis by initialising the various finite element (pile) and boundary element (soil) matrices. To predict the settlement of piles affected by nearby tunnel construction, the model predicts the ground settlement along the length of the pile. The ground settlements are then imposed on the other end of each spring. External loading is added and the resultant stresses and displacements are output but the model.

The settlements of all nodes are predicted by solving the following equation (Klar et al., 2006);

$$\{u\} = [K]^{-1}(\{f\} + [K_{soil}]\{u_t\}) \tag{22}$$

which is derived from equation (7) above.

When $\{u\}$ is solved, the model checks every node for instances where the force is higher than the limiting capacity of the node. If so, the spring connected to the load is set to 'slip' mode where the spring is set to the limiting friction while the displacement is free to change. This is iterated until no nodes are taking more loads than it could.

3.5 Example output

The following is an example of the model's predictions. Input parameters are those found in Appendix C unless otherwise stated.

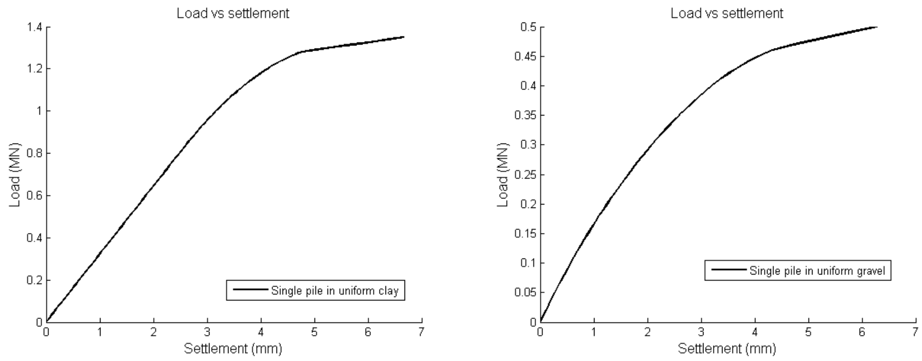

Figure 10: Simple load-displacement response of a pile in clay and sand.

Figure 10 illustrates two load-displacement plots of a pile. The plots show the gradual softening response of a pile as it is loaded to its capacity. This is consistent with expectations.

Note that the curve is linear when under low loading in the case where the pile is installed in clay. However, when the pile is in gravel, the curve is non-linear from the start. This is because pile shaft capacity in drained cases is dependant upon the effective stresses of the surrounding soil (section 3.2). Since the soil near the surface experiences negligible effective stress, the nodes reach their capacity as soon as any notable load is applied, thus leading to the early softening of the the pile response.

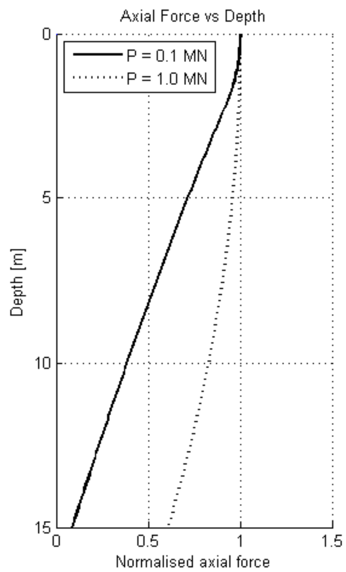

Figure 11: Comparison of axial forces within a pile at different applied loads.

Figure 11 portrays the axial forces in a pile along its depth under two different loads. Under high loads, it is clear that the load is transferred to deeper soil as the soil near the top has yielded. In this case, up to about half of the load is taken by the base.

In the absence of a tunnel (figure 12), the pile head and pile toe experience different levels of settlement. This shows that the model is able to take into account the compress-

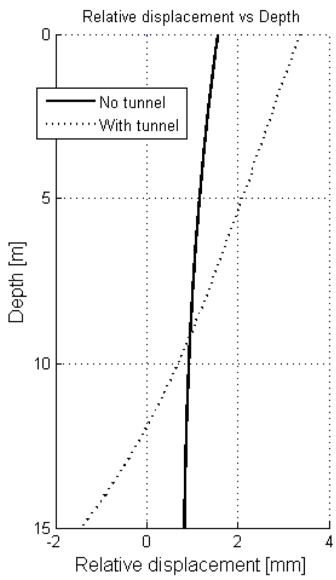

Figure 12: Relative displacement of pile along its length, with and without tunnel.

ibility of concrete. A non-linear curve also demonstrates that the shaft friction decreases with depth (steeper at the top).

Where a tunnel is positioned directly underneath the pile, the model predicts a significant settlement of the pile near the surface. Furthermore, there is also some negative relative displacement at the pile toe. This is expected as the tunnelling-induced ground settlement increases with depth. Consequently, there is a negative relative displacement near the pile toe, as the ground settles more than the pile. This inevitably leads to a loss in pile base load, and the pile will have to settle more to mobilise higher shaft friction at shallower depths, resulting in a greater relative settlement.

A gradual decrease in axial force is expected in the case where a tunnel is absent (figure 13). This shows that the load is taken gradually by shaft friction. On the other hand, it is seen that tunnelling had caused the lower half of the pile to go into tension. A negative axial force gradient indicates negative shaft friction at the lower quarter of the pile. This is expected because the pile experiences a negative displacement relative to the ground. The much greater gradient at the top half of the pile is also consistent with expectations, as the pile has to mobilise higher shaft friction to support not only the load above, but also the induced tension at the bottom.

4 Numerical investigation

This section reports the results from a series of parametric tests on the simplified model. The tool is first tested parametrically for a pile's load-displacement behaviour. It is then given different tunnel parameters to examine the resulting settlement troughs. This is followed by a study of the effects of tunnelling on existing piles.

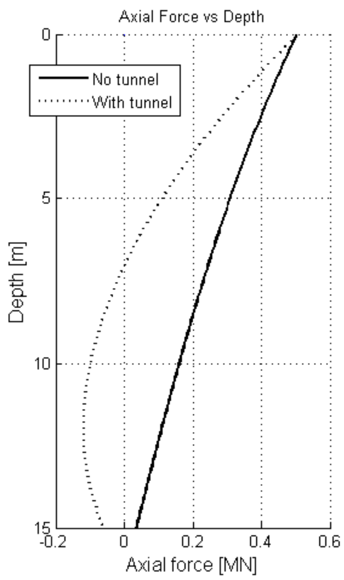

Figure 13: Comparison of axial forces within a pile, with and without tunnel. Tested with the same parameters as in figure 12.

4.1 Single pile analysis

Klar et al. (2006) monitored the response of a test pile in clay using fibre optics. After analysis, the BOTDR readings provide a continuous description of strains along the length of the pile. In this subsection, the findings of Klar et al. are compared against the predictions of the model. Details of the soil condition and pile properties are given in Appendix D.

Figure 14 illustrates the strains measured in the test pile under three successively increasing loads. There are two kinks near the upper third of the pile. This is due to changes in soil condition with depth. The strains are matched by the predictions from the model (figure 15)[1].

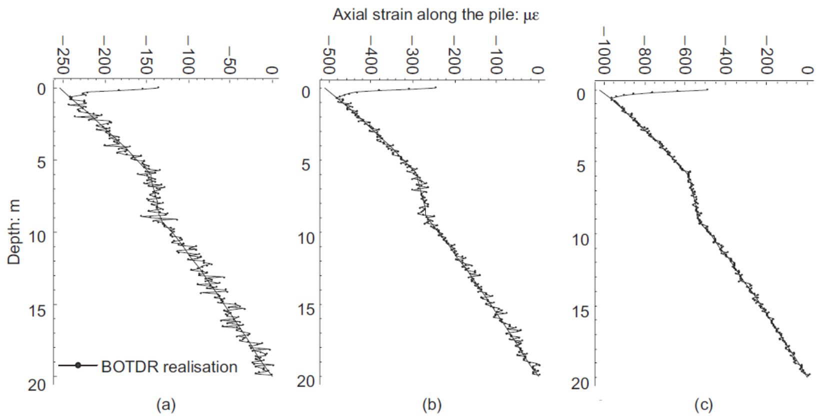

Figure 14: Strains in a pile, which is loaded to (a) 1.5 MN, (b) 3.0 MN, and (c) 6.0 MN.

[1] Strain in element i is found by $\varepsilon_i = (u_{i-1} - u_i)/L_e$

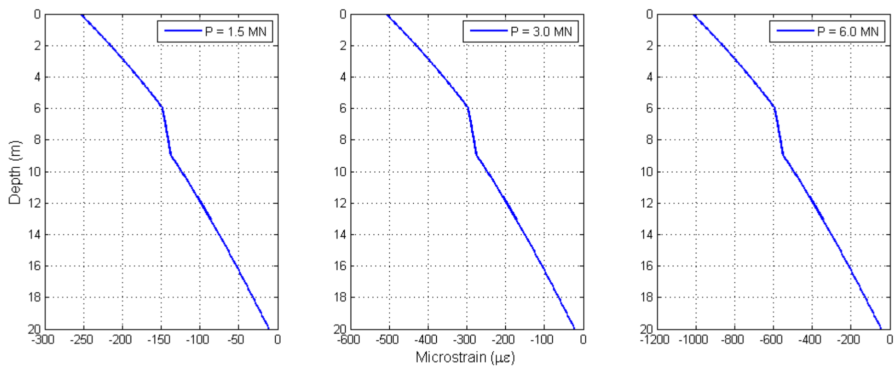

Figure 15: Strains in a loaded pile as predicted by analysis tool.

The results confirm that the numerical model is able to offer a fairly accurate prediction.

4.2 Parametric analysis of single pile settlements

This subsection investigates the settlement of piles and the various parameters that bear an effect on pile performance. In this subsection, tunnels are not included in the analysis.

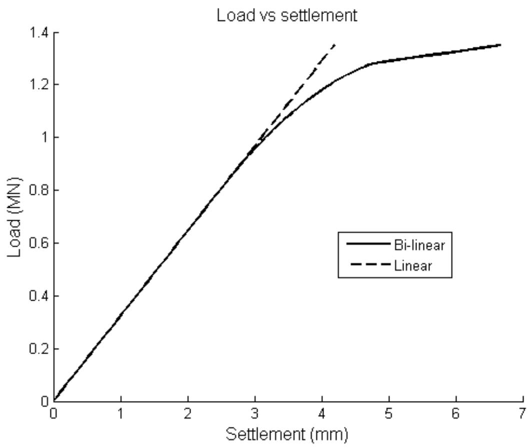

Figure 16: Load-displacement curve of a 0.5m diameter, 15m long pile.

Figure 16 compares two models: elastic (linear) and elastic-plastic(bi-linear). The bi-linear model incorporates a limiting capacity for each node, which if exceeded causes the node to slip. Other parameters are equal as between the two models. As the linear model does not have the limit imposed, the settlement continues to increase linearly with load.

In the case of the bi-linear model, the load-displacement curve is exactly the same with the linear model. It starts to deviate from linearity as soon as the first node slips, and the pile response gets progressively softer as more nodes yield. This carries on until all the shaft nodes have yielded and from this point onwards, any additional loading is transferred directly to the base, until it also fails. When it does, the pile fails.

The prediction is consistent with the behaviour of real piles.

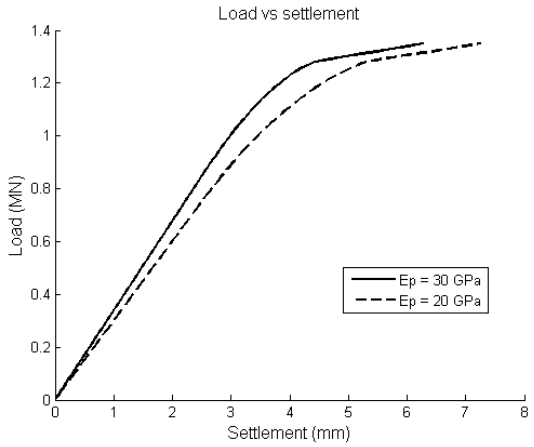

Figure 17: The effects of varying pile stiffness.

Figure 17 exhibits how the pile stiffness affects the load settlement behaviour of a pile. The curves deviate as soon as the load is applied. The stiffer pile deviates from linear response at around 1 MN, about 10% higher than the other pile. From this point onwards, the stiffer pile suffers significantly less settlement compared to the softer one. However, both piles failed at the same ultimate load, albeit at different settlements.

Typical in-situ concrete has an elastic modulus of about 25–30 GPa, and this value could drop by a third after initial shrinkage and creep effects. Lower stiffness causes significantly more settlement, especially at higher loading. Hence, it is important to have the correct pile stiffness before performing an analysis. This could pose a challenge when attempting to predict the settlements of an existing building.

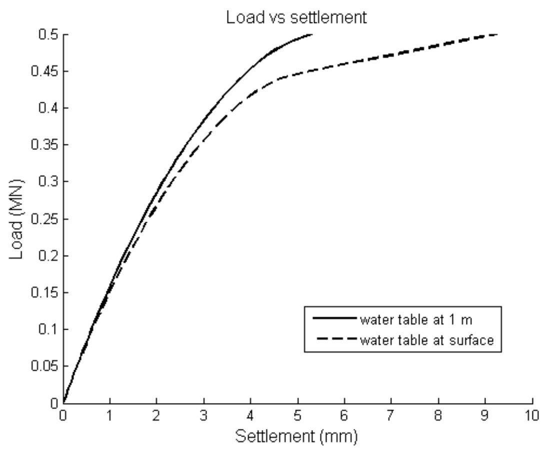

Figure 18: The effects of varying water table depth.

Figure 18 illustrates the comparison of load-displacement characteristics of two piles in gravel. One pile is located in a ground where the water table is at a depth of 1 m, whereas for the other pile the water table is positioned at the surface. The two piles display give similar displacements at low loads and begin to diverge significantly as the pile capacity of the weaker pile (where the water table is at the ground surface) is reached. This is expected as the capacity of piles in sands and gravels depends on the effective stress of the surrounding soil. A high water table will considerably reduce the effective stress in the soil and hence its bearing capacity.

An accurate estimate of the depth of the water table is needed to correctly predict the settlement of the pile. After a heavy shower, the water table might rise significantly and heavily influence the bearing capacity of soils. As such, water table estimation must be conservative.

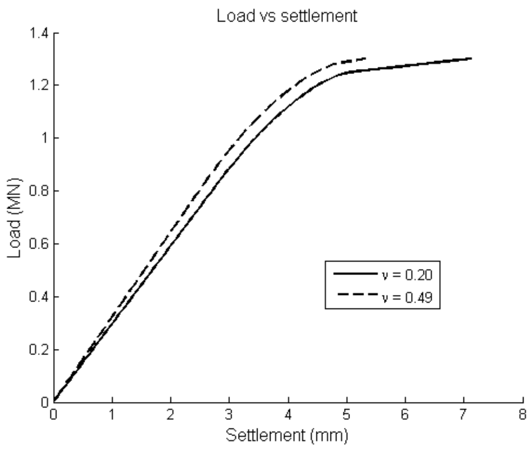

Figure 19: The effects of varying Poisson's ratio.

Figure 19 depicts the effect of changing the Poisson's ratio of the soil. For undrained analysis, ν of 0.5 is used. This is because water is incompressible. The result is a stiffer pile response. The difference is small under small loading, but increases dramatically as the pile is loaded to failure.

0.50 was not used as ν because it may cause error when used in one of the elastic modulus conversion formulae. Instead, 0.49 is used, being a value virtually identical to 0.50.

These parametric studies on single piles have yielded the following conclusions:

- The predicted behaviour of piles are qualitatively correct.
- Modelling the pile-soil interface with a bi-linear spring can predict the pile softening response.
- The pile stiffness must be determined correctly if the pile loading is expected to be close to its capacity.
- For drained analysis, the depth of the water table will affect pile behaviour significantly.
- The Poisson's ratio ν is an important parameter where the pile is heavily loaded.

4.3 'Greenfield' ground settlement due to tunnelling

This section shows the ground surface settlement due to tunnelling in 'greenfield' conditions as generated by the model (through empirical Gaussian relations). Four parameters affect the shape and size of the settlement trough: tunnel axis depth, tunnel radius, volume loss, and soil type.

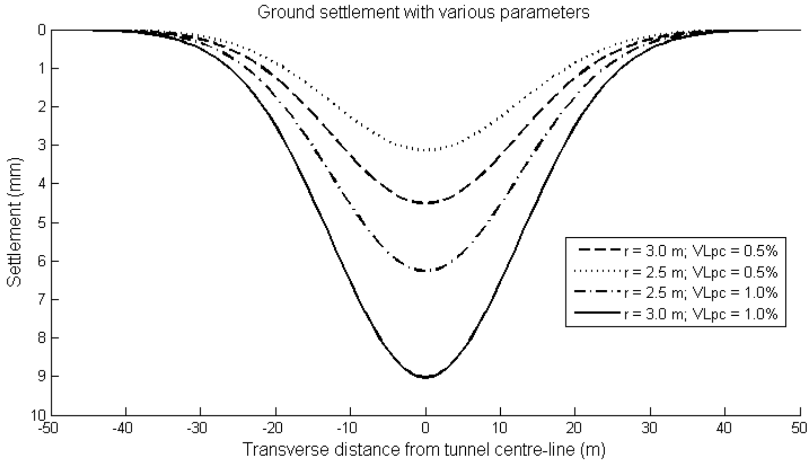

Figure 20: Parameters varied: tunnel radius and volume loss.

In figure 20, two parameters are varied and the resulting surface settlements are plotted. In section 2.2, it is shown that varying the tunnel diameter D_t and the volume loss v_l only affects the settlement magnitude $S(x)$, without affecting the through width i. This figure demonstrated that a badly controlled excavation, i.e. high v_l, combined with a large tunnel diameter, will cause a huge surface settlement. The subsurface settlements are even larger near the tunnel crown.

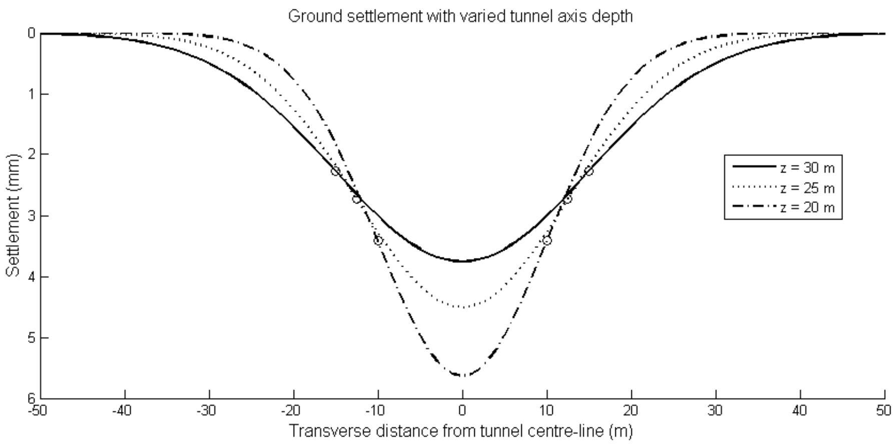

Figure 21: Change in settlement trough due to change in tunnel axis depth. Points of inflections are shifted as well (circles).

Figure 21 compares the settlement troughs caused by tunnelling at different depths. Assuming equal volume loss, a tunnel constructed closer to the surface will induce a deeper and narrower settlement trough. This is shown by the location of the point of inflection of the settlement trough. Note that the area above each curve is the same since the volume loss at the tunnel equals the volume loss at the surface. This might not be true for tunnels in sands as dilation or compaction may occur due to the movement of sand (Jacobsz, 2002).

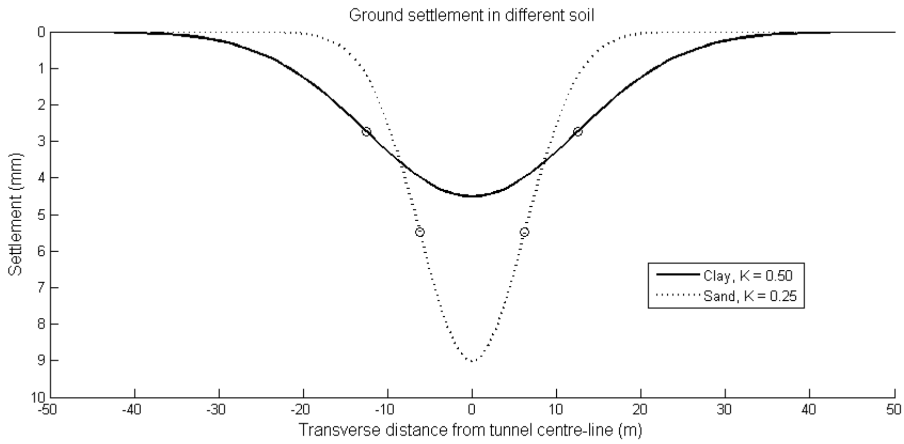

Figure 22: Change in settlement trough due to change in soil type. Points of inflections are shifted as well (circles).

Previous experience shows that tunnelling in sands cause a much narrower settlement trough as compared to tunnelling in clays. However, in grounds that contain multiple layers of sands and clays, the K value can lie somewhere inbetween 0.25 and 0.50. The model can predict the settlement profile if a K value is given. In a study by Selemetas (2005), $K = 0.42$ is back-calculated from field observations.

4.4 Pile settlement due to tunnelling effects

Selemetas (2005) proposed a three-zone influence guide (figure 6). The influence zones describe the likely settlements of piles due to tunnelling-induced ground movements. It is suggested the piles in Zone A will settle more than the 'greenfield' surface settlement, while piles in Zone C will settle slightly less than the 'greenfield' settlement. Piles in Zone B are expected to settle as much as the ground does.

The study also presented a curve, called relative vertical displacements along a transverse across the tunnel (figure 23). Relative vertical displacements (RVD) are defined as the vertical displacements of piles relative to the ground surface due to tunnelling-induced effects.

Numerical simulation by the model (figure 24) agrees with field observations qualitatively, i.e. RVD > 0 at C, RVD $= 0$ at B, and RVD < 0 at A. Quantitatively, RVD values differ by a small degree. This is because the presented plot (Selemetas, 2005) is meant to describe only the specific case monitored; the study did not propose a general equation to describe the outcomes.

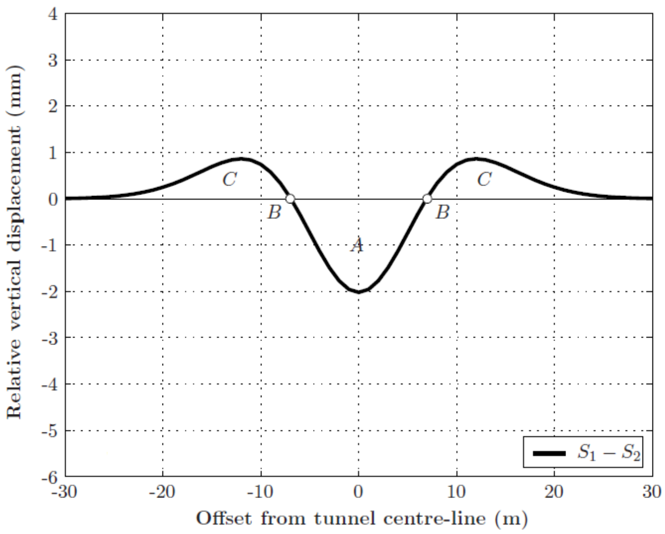

Figure 23: Field observation of relative vertical displacements (Selemetas, 2005).

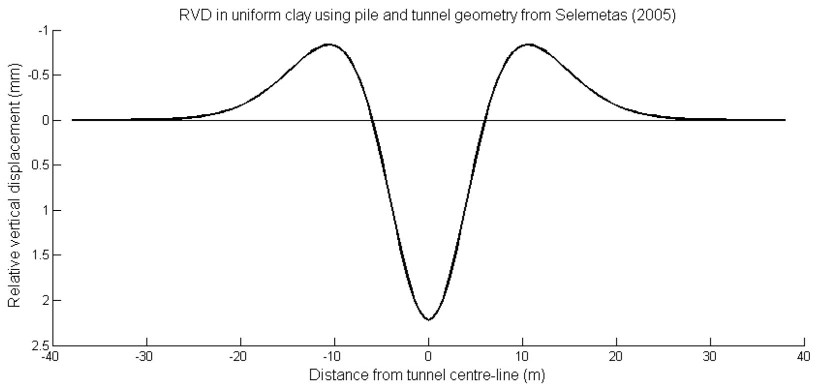

Figure 24: Model prediction of relative vertical displacements.

Additionally, the prediction is different because the model only considered a single layer of clay with uniform strength. In contrast, the piles in Selemetas' study are located in layered soil as described in Appendix B. This is in order to avoid non-cohesive granular material, i.e. made ground and terrace gravel, which needs to be modelled using the β-method. The method is proven not to be an accurate model in section 4.5.

Parametric study

The following explores parametrically the effects of tunnelling on nearby piles. In this section, the parameters used are provided in Appendix C unless specified otherwise.

Figure 25 displays the prediction of RVD values as generated by general parameters. This shows the three regions where the relative pile settlement varies from RVD>0 to RVD$=0$ and then RVD<0, i.e. the A, B, and C Zones proposed by various studies (section 2.3). Far away from the tunnel, the curve decays to zero as the ground movement due to tunnelling drops to negligible values.

Figure 26 shows how the forces within a pile evolves as the distance to tunnel centre-

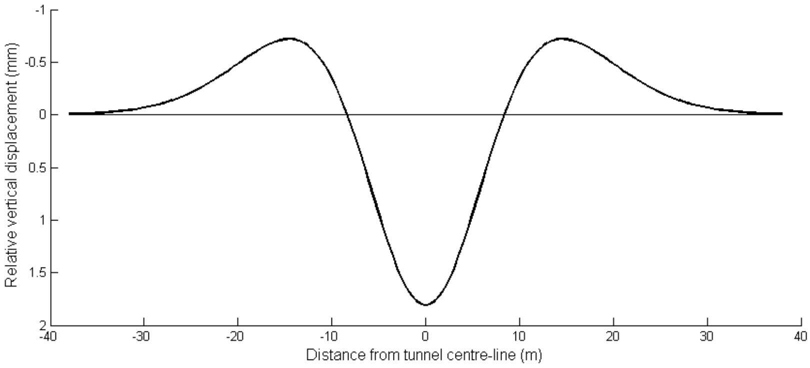

Figure 25: RVD along a transverse across the tunnel.

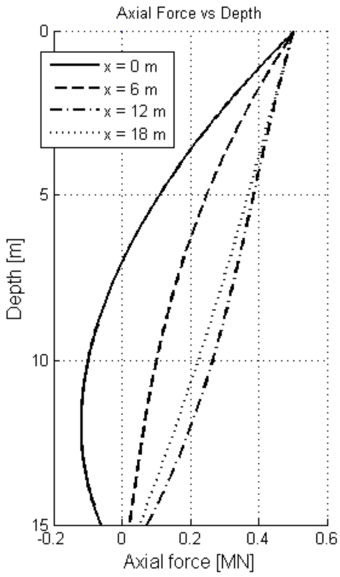

Figure 26: Comparison of axial forces within a pile located at various distances from the tunnel centre-line.

line is varied. Right above the tunnel, significant tension is introduced in half of the pile. As the distance increases, more and more of the axial load is transferred further down along the pile, up to a point where more load is taken by the base as compared to a case where no tunnel is present. These phenomena are in accordance with expectations. When the pile is right above the tunnel, deeper soil settles much more than shallow soil. This has the effect of 'dragging' the pile downwards, introducing tension to the pile. Slightly further away, shallow soil and deep soil settles by approximately the same magnitude, allowing the pile to settle by about the same magnitude as well i.e. the distance at which zone B is reached. Further away, shallow soil settles slightly more than deep soil, reducing the mobilised friction near the pile head and causing more load to be transferred to the pile toe.

Large tunnelling volume losses cause larger displacements, especially near the tunnel crown. Piles extend all the way down, thus larger displacements deep underground cause

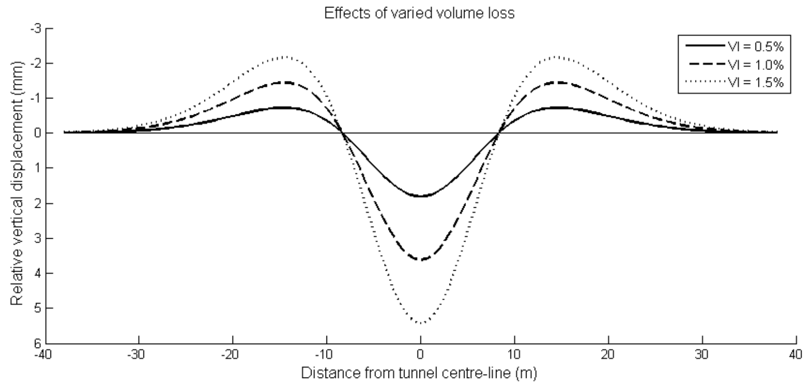

Figure 27: Effects of varying volume loss.

larger pile head settlements.

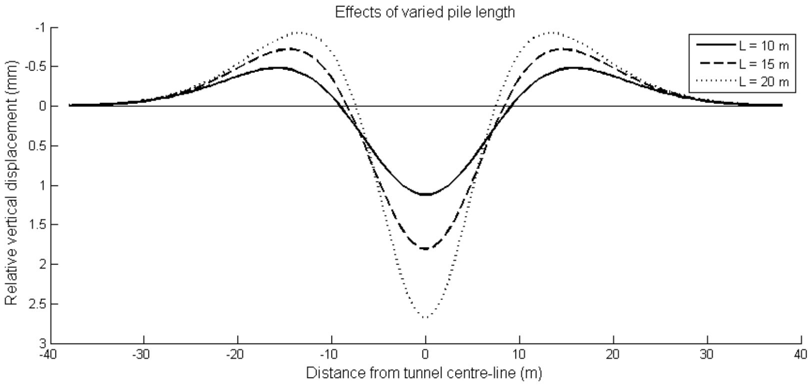

Figure 28: Effects of varying pile length.

The effects of varying pile length (figure 28) are similar, albeit with a notable difference. At the centre-line, longer piles suffer from much larger RVDs. This is unsurprising because longer piles reach deeper levels of soil, where the settlement is much larger. With larger settlements, the longer piles are affected more and the result is a greater RVD.

The difference is that the point at which the RVD curves cross 0 is not the same. In the previous case (figure 27), all the RVD curves cross the x-axis at the same point. Both results are as expected.

The geometry of the piles and the tunnel is the same for the case in figure 27; conversely, it changes according to the pile length for the case in figure 28. In deeper soil, the subsurface settlement is narrower. Consequently, the pile toe of a longer pile will cross the B-line at a closer distance compared to shorter piles. As a result, the RVD curves of longer piles cross the x-axis at a distance closer to the tunnel. This is consistent with the concept of influence zones.

Figure 29 compares and contrasts the axial loads within piles of different lengths. The response of the piles at three different distances from the tunnel centre-line are compared as well.

The first sub-figure shows the axial forces in three piles of different lengths situated

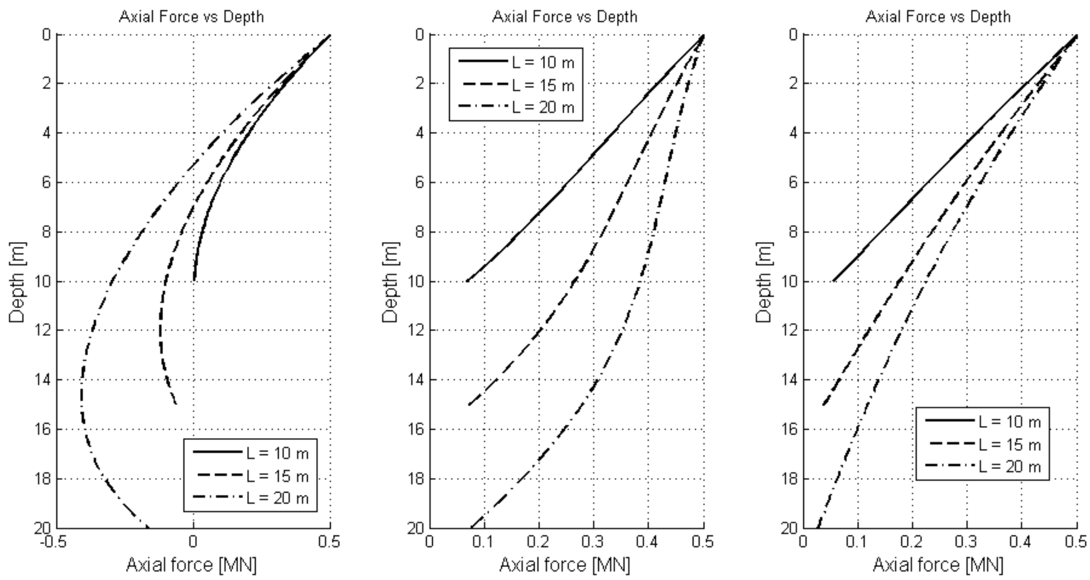

Figure 29: Axial loads in piles of various lengths at different distances from tunnel centre-line: 0 m, 12 m, and 24 m.

right above the tunnel. It has been shown in figure 28 that longer piles suffer from larger RVDs. From this sub-figure, it could be seen that the longest pile suffers from significant negative shaft friction near the pile base, bringing much of the pile into tension. The shortest pile did not experience tension; however it is obvious from the curvature of the graph that the pile toe carries almost zero load, through the shaft as well as the base.

In the second sub-figure, the piles are located 12 m from the tunnel centre-line. From the curvatures, the longer piles have more of their load transferred to deeper soil. This is expected as the piles are now in zone C, where the ground is expected to settle more than the pile head does. As the settlement trough near the surface is wider, is manages to reach the piles 12 m away. Deeper settlement troughs are much narrower, hence the soil near the pile toes of the longer piles 12 m away does not experience any significant settlement. As the soil near the surface settles more than the pile does, less friction is mobilised. This causes the pile to transfer more load to the deeper area.

At 24 m from the tunnel, the piles are sufficiently far away to not be heavily affected by the tunnel construction. The third sub-figure shows that three of the piles behave as if there are no tunnelling-induced effects.

Figure 30 compares the RVD curves as the tunnel depth is varied. From the graph, it is noted that the shape of the curve narrows and gets deeper for a shallower tunnel. This is expected. A deeper tunnel will result in relatively shallower displacements and a wider settlement trough. Besides that, the point where the RVD curves cross the x-axis, which is also the transition from zone A to zone C, is different. This can be explained by the fact that the trough width is directly affected by the tunnel depth.

Figure 31, compares the axial loads in piles installed at different distances away from

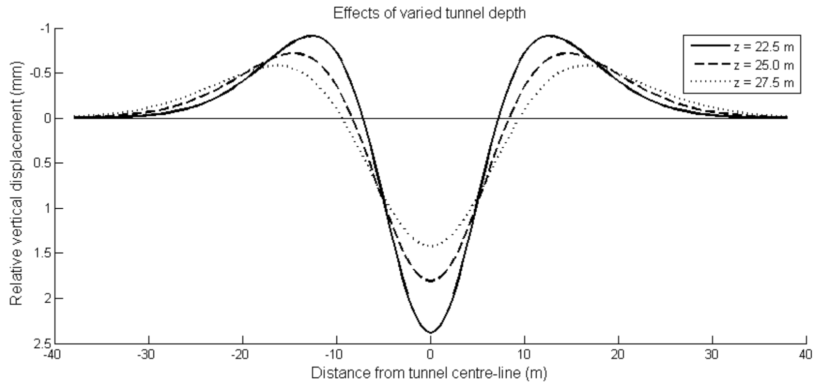

Figure 30: Effects of varying tunnel depth.

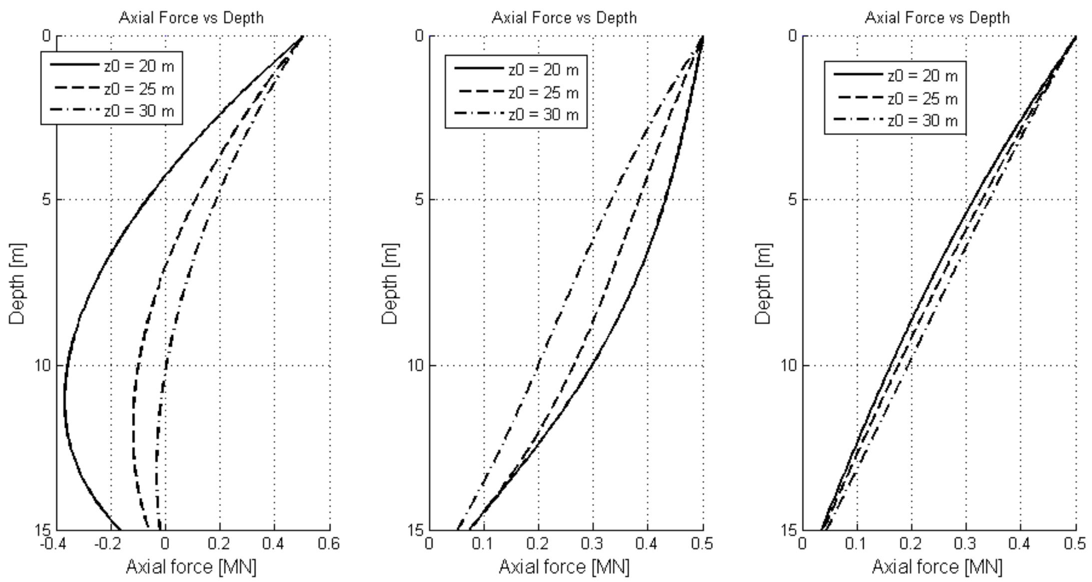

Figure 31: Axial loads in piles of various lengths at different distances from tunnel centre-line: 0 m, 12 m, and 24 m.

the tunnel. The figure contrasts the axial forces induced by tunnels at different depths.

In the first sub-figure, it can be seen that a shallow tunnel causes unbearably high tension in the pile, up to almost the imposed loading, in tension. In the case of a deep tunnel, the area of high settlements right above the tunnel crown is sufficiently far away from the pile toe. Therefore deeper tunnels cause less extreme changes to a the stresses of a pile.

At 12 m away from the tunnel, the second sub-figure shows that the pile with a shallow tunnel is mobilising more shaft friction at the lower end of the pile, indicating that the pile is already in zone C. On the other hand, the pile with the deeper tunnel showed a relatively uniform transfer of load along the length of the pile, suggesting that the pile is in zone B.

At 24 m, the different tunnels did not lead to any significant difference in the pile stresses. This shows that the piles are all sufficiently far away from the effects of tunnelling-induced ground movements.

It was found that varying s_u and the applied load does not affect the RVD curves of the pile as long as the load does not exceed the pile capacity.

4.5 Comparison with field data

In this subsection, the model is validated against the findings of Selemetas (2005), whose study was chosen because of the high quality of its research measurements. In the study, four instrumented test piles were installed at a strategic location to investigate the influence zones proposed by Jacobsz (2002).

The piles (bored piles) are loaded to half of the designated capacity before the tunnel boring machines (TBM) arrive. Settlements of the ground and pile heads as well as strains in the piles are monitored closely as the twin tunnels are being constructed beneath the piles. A borehole is used to extract soil samples at the area. Relevant parameters are listed and tabulated in Appendix B.

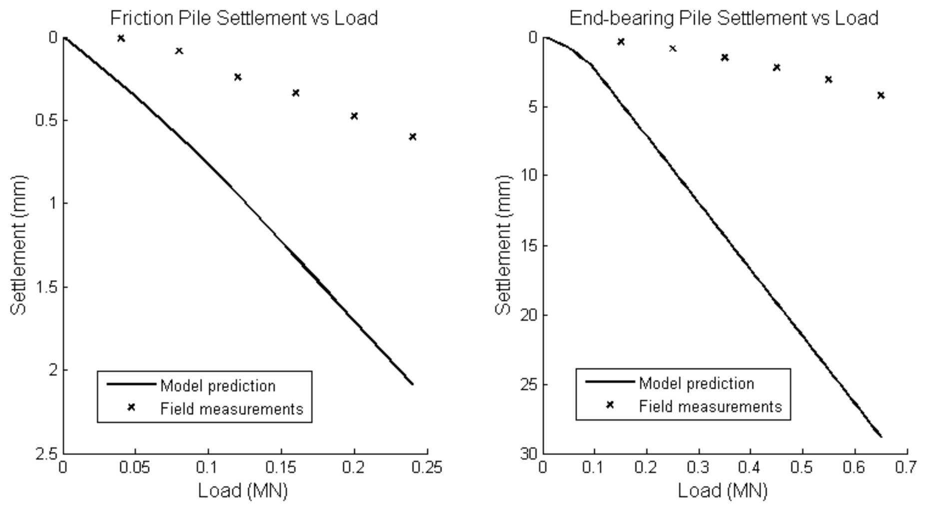

Figure 32: Comparison of pile head settlement due to axial load. Field measurements from Selemetas (2005).

Figure 32 shows a comparison between field data and predictions from the model. The loading of the test piles is done in stages to allow for soil consolidation. The model predicted 4–6 times more settlement compared to field data.

In order to investigate the cause behind the discrepancies, the predicted axial loads within the piles are compared side by side against field observations (figures 33 and 34).

From the comparisons, it is found that the predicted capacity of the Made Ground layer is much lower than the actual mobilised strength of the layer found in the actual piles. Checking the states of the nodes further revealed that all nodes located in the Made Ground layer and Terrace Gravel layer have slipped.

In the predicted results, the top 3 m of the shaft mobilised around 22 kN of force.

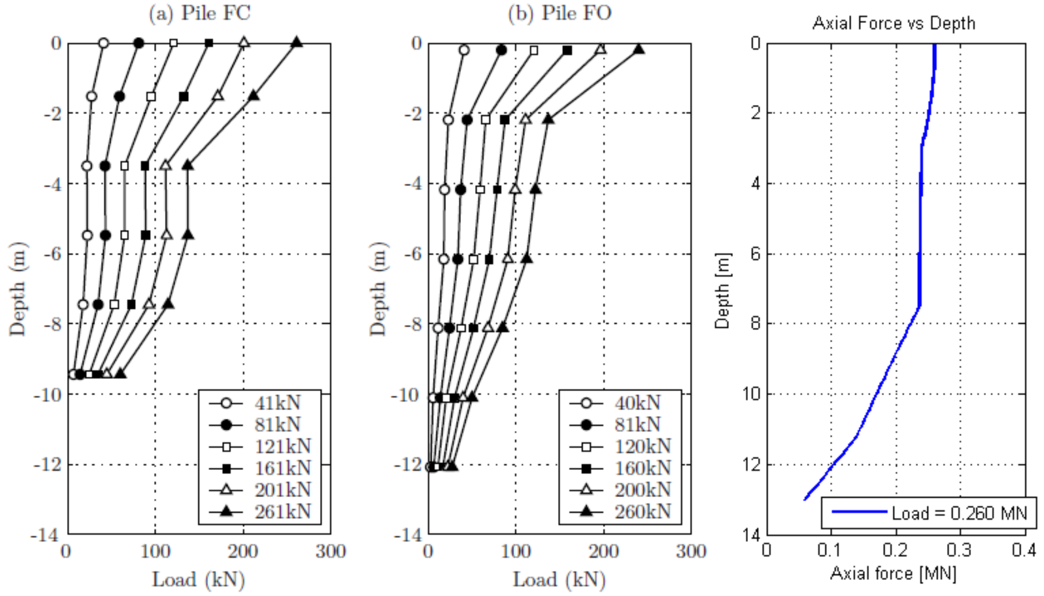

Figure 33: Comparison of Pile F axial loads.

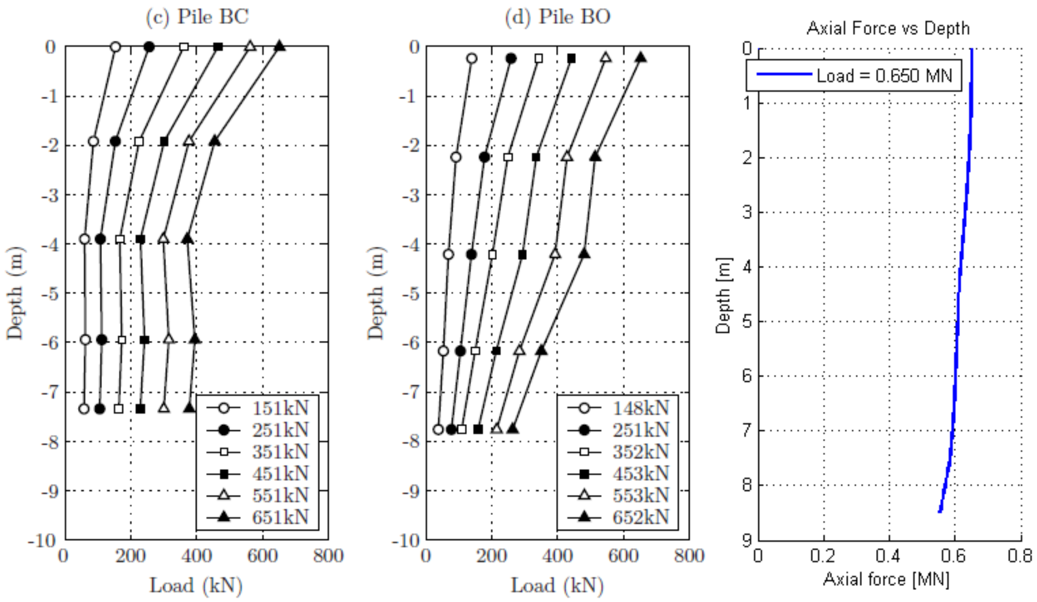

Figure 34: Comparison of Pile B axial loads.

In contrast, the actual piles studied managed to mobilise 130 kN in that layer. The pile shaft capacity of the top 3 m is calculated using the β-method:

$$Q_s = 2\pi r_p L \times K_0 \sigma'_{v0} \tan(\delta) \tag{23}$$

with $r_p = 0.24\,\mathrm{m}$, $L = 3\,\mathrm{m}$, $K_0 = 0.6$, $\delta = 0.75\,\phi' = 0.75 \times 22°$, and $\sigma'_{v0} = 27\,\mathrm{kN/m^2}$. [2]

$$\begin{aligned} Q_s &= 2 \times 3.14 \times 0.24 \times 3 \times 0.6 \times 27 \times \tan(0.75 \times 22°) \\ &= 21.7\,\mathrm{kN} \end{aligned} \tag{24}$$

which matches the model prediction of the shaft capacity for the first 3 m. With this finding, several inferences can be drawn:

- The β-method might not be the relevant method to use in this case.
- Some uncertainties may be involved in the soil parameters, e.g. the K_0 and ϕ' value.
- The Made Ground layer is thicker than expected. However, this is highly unlikely as field observations indicated a big drop in shaft friction around the 3 m depth, where the soil makes a transition from Made Ground to Alluvium.
- The β-method does not seem to provide sufficient capacity, assuming the parameters are accurate. This implies that there might be additional ways in which the soil managed to provide friction. Nevertheless this is unlikely, for the β-method is a well researched and tested method.

4.6 Discussion

- Numerical model provides good prediction for single pile analysis.
- In case of non-cohesive soil which requires the adoption of β-method, the match is not perfect.
- Relative settlements between pile and 'greenfield' is in qualitative agreement with field data.
- This method needs to be refined and extended to overcome the known limitations. Such shortcoming is the input of 'greenfield' tunnel settlements on the pile which ignore real tunnel-pile interaction that results in smaller settlement than in 'greenfield'. It is recommended that in the future new relations for tunnel settlements are adopted that consider the presence of piles and therefore are more suitable than the 'greenfield' ones.

5 Conclusion

The following conclusions are drawn from this study:

[2] Depth of water table is 4 m, for soil depth of 0–3 m, $\gamma' = \gamma = 18\mathrm{kN/m^3}$. Therefore average vertical stress $= 18 \times 3/2$.

- The simplified model is able to predict the strains in a single vertically loaded pile installed in clay reasonably well.
- The is a potential limitation in the model's implementation of the β-method when analysing piles in Made Ground. Further work is needed to overcome the challenge of modelling non-cohesive granular soil accurately.
- The model's predictions of relative vertical settlements agree well qualitatively with the observed trends. However, the exact quantitative validation was not possible due to limitations of the model to accurately model pile-soil interaction in a non-cohesive granular material.
- For tunnelling-induced pile settlements, the bi-linear elastic-plastic model used to define the pile-soil interface could be improved by adopting a non-linear cyclic load transfer approach model. This is due to the fact that some of the nodes experience load reversal, i.e. changing from positive shaft friction to negative shaft friction.
- The simplified model ignores the real tunnel-pile interaction, i.e. the 'greenfield' ground settlement is imposed on the piles. The real ground settlements is probably less due to the soil stiffening effects by the piles.
- The model is sensitive towards some of the input parameters, thus there is a need to ensure that the parameter values match the real world values.

6 Recommendations for future work

This section highlights the areas in which future work can focus on.

- The first and foremost issue is to model the pile shaft capacity accurately for pile nodes that are located in a layer consisting of sand/gravel.
- Model cases where the pile toe is deeper than the tunnel. This requires a model that could predict the tunnelling-induced subsurface settlement under the tunnel axis.
- Validate the model with more test results — FEM ((Chen et al., 1999)), centrifuge testing ((Jacobsz, 2002); (Farrell, 2011); (Loganathan et al., 2000)), field observations ((Sirivachiraporn and Phienwej, 2012)), 1g experiment ((Meguid and Mattar, 2009)).
- Model the response of pile groups. For a simplified approach, the pile-soil-pile interaction can be modelled using Mindlin's elastic solution (Kitiyodom et al., 2005).

- Include the horizontal component of the tunnelling induced settlement. Extensive field data is available for validation, e.g. Selemetas (2005). This means that the bar elements used to model the piles need to be converted into beam elements. Beam elements can take shear forces and bending moments as well as axial loads. With this, the model will be able to model foundations that take lateral loads, e.g. wind.
- Use a hyperbolic (non-linear) curve instead of an elastic-plastic (bi-linear) response for the springs describing the pile-soil interaction (Boscardin et al., 1990). This can model the interaction better, but will be more computationally intensive.
- Model the loss of capacity of piles in cases where the piles suffer significant base load losses, i.e. above the tunnel. The current model only predicts settlements.
- To implement a simplified model to predict the reduction of tunnelling-induced ground settlement due to the soil stiffening effects of pile groups and large structures.
- Model the behaviour of driven piles, which suffers from locked in stresses. The loss of capacity must be modelled (Marshall and Mair, 2011).
- Implementing the tunnelling-induced settlement in front of the TBM (in the shape of a cumulative distribution) will allow the prediction of differential settlement in a structure as the TBM is advancing near the structure. Further improvements can be made to model the heaving of ground due to slurry pressure and tail grouting from the TBM.
- Model the soil as an anisotropic material. Analytical solutions have been presented by Zymnis et al. (2013) and Puzrin et al. (2012).
- Under-reamed piles are designed to have a higher capacity due to the enlarged pile base. However, tunnel construction causes much larger settlement at the base of a pile. This is a potential area to be investigated.

7 Acknowledgements

I am indebted to Dr. Yan J. for his kind support and supervision throughout the year. My gratitude extends to Dr. L. Pelecanos, whose guidance has been invaluable to this project, as well as Prof. K. Soga and Dr. Xu X. for their assistance and advice.

8 Appendix

Appendix A

Risk assessment review

A risk assessment is conducted at the start of the project. The aim of the assessment is to identify hazards and take precautionary measures to reduce the chances of the hazards materialising.

As this project focuses mainly on numerical analysis, almost all of the time will spent by the author in front of the computer. Key risks include injuries from bad posture and eye strain. These can be eliminated by adopting a correct posture and taking breaks.

By the end of the project, none of the hazards were encountered.

Appendix B

Model input parameters when simulating the findings of Selemetas (2005):

$$z_0 = 19 \text{ m}$$
$$D_t = 8.15 \text{ m}$$
$$v_l = 0.2 \ \%$$
$$D_p = 0.48 \text{ m}$$
$$E_p = 23.4 \text{ GPa}$$
$$\text{Pile F, } L = 13 \text{ m, loaded to 240 kN}$$
$$\text{Pile B, } L = 8.5 \text{ m, loaded to 650 kN}$$

	Depth (m)	γ (kN/m^3)	G (MPa)	K_0	s_u (kPa)	ϕ_{peak}	ϕ_{crit}
Made Ground	0–3.0	18	10	0.6	–	22°	22°
Clay	3.0–4.1	15	0.3	0.6	20	20°	20°
Peat	4.1–6.6	15	0.15	0.6	20	20°	20°
Clay	6.6–4.7	15	0.3	0.6	20	20°	20°
Terrace Gravel	7.5–11.2	20	10	0.4	–	39°	36°
London Clay	11.2–	19	18	–	$60 + 10z$	26°	20°

Table 2: Soil parameters

Appendix C

Piles are modelled in a layer of clay unless stated otherwise. Input parameters for parametric studies:

$$
\begin{aligned}
P &= 0.5\,\mathrm{MN} \\
E_{pile} &= 25\,\mathrm{GPa} \\
L_{pile} &= 15\,\mathrm{m} \\
D_{pile} &= 0.5\,\mathrm{m} \\
L_e &= 0.1\,\mathrm{m} \\
z_0 &= 25\,\mathrm{m} \\
r_t &= 3\,\mathrm{m} \\
v_l &= 0.5\,\% \\
G_{soil} &= 20\,\mathrm{MPa}, \text{ in clays} \\
&= 10\,\mathrm{MPa}, \text{ in sand/gravel} \\
\gamma_{soil} &= 20\,\mathrm{kN/m^3} \\
K_0 &= 0.4 \\
\phi_{peak} &= 39^\circ \\
\phi_{crit} &= 36^\circ \\
s_u &= 100\,\mathrm{kPa} \\
\alpha &= 0.5 \\
\nu &= 0.49 \text{ in clays} \\
&= 0.20 \text{ in sand/gravel}
\end{aligned}
$$

ν is taken as 0.49 because 0.5 (in undrained cases) will cause error when used in the equation $K = E/3(1-2\nu)$. The water table is set to be at the ground surface.

Appendix D

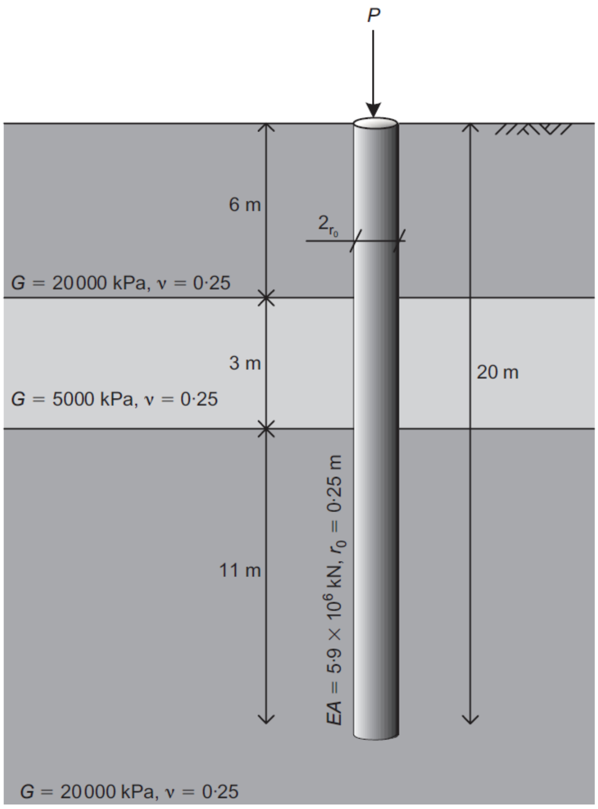

Figure 35: The pile and soil properties from Klar et al. (2006).

References

Addenbrooke, T., Potts, D., and Puzrin, A. (1998). The influence of pre-failure soil stiffness on the numerical analysis of tunnel construction. *Pre-failure Deformation Behaviour of Geomaterials*, page 307.

Attewell, P. B., Yeates, J., and Selby, A. R. (1986). Soil movements induced by tunnelling and their effects on pipelines and structures.

Bakker, K., De Boer, F., Admiraal, J., and Van Jaarsveld, E. (1999). Monitoring pilot projects using bored tunnelling: the second heinenoord tunnel and the botlek rail tunnel. *Tunnelling and Underground Space Technology*, 14(2):121–129.

Boscardin, M. D., Selig, E. T., Lin, R.-S., and Yang, G.-R. (1990). Hyperbolic parameters for compacted soils. *Journal of Geotechnical Engineering*, 116(1):88–104.

Chen, L., Poulos, H., and Loganathan, N. (1999). Pile responses caused by tunneling. *Journal of Geotechnical and Geoenvironmental Engineering*, 125(3):207–215.

Cheng, C., Dasari, G., Chow, Y., and Leung, C. (2007). Finite element analysis of tunnel–soil–pile interaction using displacement controlled model. *Tunnelling and Underground Space Technology*, 22(4):450–466.

Chow, Y. (1986). Analysis of vertically loaded pile groups. *International Journal for Numerical and Analytical Methods in Geomechanics*, 10(1):59–72.

Cording, E. J. and Hansmire, W. (1975). *Displacements around soft ground tunnels.*

Coutts, D. and Wang, J. (2000). Monitoring of reinforced concrete piles under horizontal and vertical loads due to tunnelling. *Proceedings of Tunnels and Underground Structures, London*, pages 514–546.

Craig, R. F. (2004). *Craig's soil mechanics.* CRC Press.

Farrell, R. (2011). *Tunnelling in sands and the response of buildings.* PhD thesis, University of Cambridge.

Jacobsz, S. (2002). The effects of tunnelling on piled foundations. *Geotechnical Department. Cambridge, University of Cambridge. Doctor of Philosophy.*

Jongpradist, P., Kaewsri, T., Sawatparnich, A., Suwansawat, S., Youwai, S., Kongkitkul, W., and Sunitsakul, J. (2013). Development of tunneling influence zones for adjacent pile foundations by numerical analyses. *Tunnelling and Underground Space Technology*, 34:96–109.

Kitiyodom, P., Matsumoto, T., and Kawaguchi, K. (2005). A simplified analysis method for piled raft foundations subjected to ground movements induced by tunnelling. *International journal for numerical and analytical methods in geomechanics*, 29(15):1485–1507.

Klar, A., Bennett, P. J., Soga, K., Mair, R. J., Tester, P., Fernie, R., St John, H. D., and Torp-Peterson, G. (2006). Distributed strain measurement for pile foundations. *Proceedings of the ICE-Geotechnical Engineering*, 159(3):135–144.

Klar, A., Spasojevic, A., and Soga, K. (2004). Continuum solution of lateral loading of large pile groups. *Technical Rep. No. CUED/D TR*, 334.

Klar, A., Vorster, T., Soga, K., and Mair, R. (2007). Elastoplastic solution for soil-pipe-tunnel interaction. *Journal of geotechnical and geoenvironmental engineering*, 133(7):782–792.

Kraft, L. M., Kagawa, T., and Ray, R. P. (1981). Theoretical tz curves. *Journal of the Geotechnical Engineering Division*, 107(11):1543–1561.

Lee, C. and Jacobsz, S. (2006). The influence of tunnelling on adjacent piled foundations. *Tunnelling and underground space technology*, 21(3):430.

Lee, G. T. and Ng, C. W. (2005). Effects of advancing open face tunneling on an existing loaded pile. *Journal of Geotechnical and Geoenvironmental Engineering*, 131(2):193–201.

Lee, Y.-J. and Bassett, R. H. (2007). Influence zones for 2d pile–soil-tunnelling interaction based on model test and numerical analysis. *Tunnelling and underground space technology*, 22(3):325–342.

Leung, Y. (2010). *Foundation optimization and its application to pile reuse.* PhD thesis, Thesis, Cambridge University.

Loganathan, N. and Poulos, H. (1998). Analytical prediction for tunneling-induced ground movements in clays. *Journal of Geotechnical and Geoenvironmental Engineering*, 124(9):846–856.

Loganathan, N., Poulos, H., and Stewart, D. (2000). Centrifuge model testing of tunnelling-induced ground and pile deformations. *Geotechnique*, 50(3):283–294.

Loganathan, N., Poulos, H., and Xu, K. (2001). Ground and pile-group responses due to tunnelling. *Soils and Foundations*, 41(1):57–67.

Mair, R. and Taylor, R. (1997). Bored tunnelling in the urban environment. 14th int. In *Conf. SMFE, Hamburg*.

Mair, R., Taylor, R., and Bracegirdle, A. (1993). Subsurface settlement profiles above tunnels in clays. *Geotechnique*, 43(2).

Mair, R. J. (1978). *Centrifugal modelling of tunnel construction in soft clay*. PhD thesis.

Marshall, A. (2009). Tunnelling in sand and its effect on pipelines and piles. *London: University of Cambridge*.

Marshall, A. M. and Mair, R. J. (2011). Tunneling beneath driven or jacked end-bearing piles in sand. *Canadian Geotechnical Journal*, 48(12):1757–1771.

Meguid, M. A. and Mattar, J. (2009). Investigation of tunnel-soil-pile interaction in cohesive soils. *Journal of geotechnical and geoenvironmental engineering*, 135(7):973–979.

Mindlin, R. D. (1936). Force at a point in the interior of a semi-infinite solid. *Physics*, 7(5):195–202.

Morgan, H. and Bartlett, J. (1969). Victoria line. 3. tunnel design. In *PROCEEDINGS OF THE INSTITUTION OF CIVIL ENGINEERS*, volume 44, page 353.

Morton, J. and King, K. (1979). Effects of tunneling on the bearing capacity and settlement of piled foundations. In *Proc. Tunnelling*, volume 79, pages 57–58.

Mroueh, H. and Shahrour, I. (2002). Three-dimensional finite element analysis of the interaction between tunneling and pile foundations. *International Journal for Numerical and Analytical Methods in Geomechanics*, 26(3):217–230.

O'Reilly, M. and New, B. (1982). Settlements above tunnels in the united kingdom-their magnitude and prediction. Technical report.

Pang, C., Yong, K., Chow, Y., and Wang, J. (2005). The response of pile foundations subjected to shield tunnelling. In *5th Int'l Symposium Geotechnical Aspects of Underground Construction in Soft Ground, Balkema*.

Peck, R. B. (1969). Deep excavations and tunnelling in soft ground. In *Proc. 7th Int. Conf. on SMFE*, pages 225–290.

Poulos, H. and Davis, E. (1968). The settlement behaviour of single axially loaded incompressible piles and piers. *Geotechnique*, 18(3):351–371.

Poulos, H. G. (1989). Pile behaviourtheory and application. *Geotechnique*, 39(3):365–415.

Puzrin, A., BURLAND, J., and STANDING, J. (2012). Simple approach to predicting ground displacements caused by tunnelling in undrained anisotropic elastic soil. *Géotechnique*, 62(4):341–352.

Randolph, M. F. and Wroth, C. P. (1978). Analysis of deformation of vertically loaded piles. *Journal of the Geotechnical Engineering Division*, 104(12):1465–1488.

Sagaseta, C. (1987). Analysis of undraind soil deformation due to ground loss. *Geotechnique*, 37(3):301–320.

Selemetas, D. (2005). *The response of full-scale piles and piled structures to tunnelling*. PhD thesis, University of Cambridge.

Sirivachiraporn, A. and Phienwej, N. (2012). Ground movements in epb shield tunneling of bangkok subway project and impacts on adjacent buildings. *Tunnelling and Underground Space Technology*, 30:10–24.

Skempton, A. (1951). The bearing capacity of clays.

Takahashi, K., Fukazawa, N., Hagiwara, T., and Hosoda, M. (2004). Observational control of slurry shield tunnels with super close spacing under the nearby bridge abutments loads. *Tunnelling and Underground Space Technology*, 19:390.

Teunissen, E. and Hutteman, M. (1998). Pile and surface settlements at full scale tests north/south metroline amsterdam. In *Tunnels and Metropolises: Proceedings of the World Tunnel Congress*, volume 98, pages 981–986.

Verruijt, A. and Booker, J. (1996). Surface settlements due to deformation of a tunnel in an elastic half plane. *Geotechnique*, 46(4):753–756.

Xu, K. and Poulos, H. (2001). 3-d elastic analysis of vertical piles subjected to passive loadings. *Computers and Geotechnics*, 28(5):349–375.

Yong, K. and Pang, C. (2004). Geotechnical challenges of the mass rapid transit (mrt) system in singapore. In *Malaysian geotechnical conference*.

Zienkiewicz, O. C. and Taylor, R. L. (2005). *The finite element method for solid and structural mechanics*. Butterworth-heinemann.

Zymnis, D., Chatzigiannelis, I., and Whittle, A. (2013). Effect of anisotropy in ground movements caused by tunnelling. *Géotechnique*, 63(13):1083–1102.